A Quantum Monte Carlo Study of the Molybdenum Dimer (Mo_2)

Adem Halil Kulahlioglu*

Department of Physics, Ulsan National Institute of Science and Technology, Republic of Korea

Lubos Mitas

Department of Physics and CHiPS, North Carolina State University, Raleigh, NC 27695, USA

Abstract

We have studied the molybdenum dimer (Mo_2) system. The binding energy was calculated by means of the fixed-node DMC (FN-DMC) method. The Slater part of the trial wave function was constructed by the Selected-CI method by using the orbitals generated by the KS-DFT method with a hybrid meta-GGA exchange and correlation functional, TPSSh. We also carried out CCSD(T) calculations which were subsequently extrapolated to the complete basis set (CBS) limit. The results are presented.

Keywords: Quantum Monte Carlo, the Fixed-Node Approximation, molybdenum, Mo_2, Coupled-cluster, complete basis set limit,

1. Introduction

As a transition metal, molybdenum (Mo) often fulfills important role in electronic structure properties of a number of chemical systems. This versatility stems from its half-filled outer d-shell with significant degeneracies and tendency to form multiple bonds. These systems host a rich spectrum of many-body effects due to strong correlations so it is not surprising that they also pose challenges for theoretical studies [1–13]. Computationally efficient and popular electronic structure techniques such as Density Functional Theory (DFT) method have a mixed reliability for these types of correlated systems. Obviously, investigations by alternatives with significantly higher accuracy are highly desirable.

Mo and its isoelectron atomic counterparts (Cr and W in the group VIB) with their five nd and $(n+1)s$ orbitals form dimers (Cr_2, Mo_2 and W_2) with a high multiplicity of bonds. However, due to the different characteristics of nd orbitals, the nature of corresponding bonding varies. In particular, in Cr_2 d orbitals are more localized when compared with Mo_2. Interestingly, Cr_2 has a much smaller binding energy than Mo_2 [8] despite having much smaller bond length. This somewhat counterintuitive fact is due to the very strong electron-electron repulsion in the molecular orbitals formed mainly from the $d-$channel.

Mo_2 is a low spin-state molecule with ground state ${}^1\sum_g^+$ and it dissociates into an atomic state with maximized spin-state, ${}^7S$. Mo_2 has nominally sextuple bond with the following diatomic orbitals:

$$\sigma_g^2(d)\pi_u^4(d)\delta_g^4(d)\sigma_g^2(s). \tag{1}$$

Due to multiple degeneracies and high electron density in the bond region of Mo_2 and similar systems, their binding energy calculations have been a difficult task for ab initio methods[3]. For instance, Kohn Sham DFT gives very scattered values with different types of exchange-correlation functionals; the binding energy is biased by the choice of the functionals [13]. Also, CASSCF level methods underestimate the binding energy, often with a large degree discrepancy [14].

*Corresponding author

Email address: ahkulahl@ncsu.edu (Adem Halil Kulahlioglu)

In this paper we have aimed at calculating the binding energy of Mo_2 by using the fixed-node diffusion Monte Carlo (FN-DMC), a projector QMC method in real space of electron coordinates. FN-DMC employs a stochastic many-body methodology with sophisticated trial functions [15, 16]. Its accuracy, however, depends on the quality of the nodal structure (i.e., the sign structure) of the trial wave function since its nodes are only approximate. Our trial wave function was of a Slater-Jastrow type, i.e., a product of linear combination of Slater determinants and a Jastrow factor. Since the ground state of Mo_2 needs to be represented with a multi-referenced wave function, sufficiently extensive linear combination of Slater determinants in the trial wave function is crucial. The method is computationally demanding and most of the QMC computational is spent on evaluating the trial wave function, its gradients and laplacians [16–18]. Hence, while the trial wave function should reflect the exact wave function (or the exact nodes) to the highest possible extent, the wave function should be as compact as possible in order to achieve the optimal trade-off between the accuracy and the computational time demands.

To this end, there are determinant update methods [19] which allow us to lower the complexity of the computational time to evaluate the value, gradients and laplacian of a determinant expansion. Hence, the computational time is not necessarily linear with the number of determinants but could possibly exhibit a more favorable scaling such as $\sqrt{N_{\rm det}}$ [20], where $N_{\rm det}$ is the number of determinants.

Fortunately, FN-DMC usually converges much faster than CI type methods regarding the number of determinants, provided that the most significant determinants are included in the expansion. For instance, in Ref. [21], it was demonstrated that FN-DMC was able to account 98-99% of the correlation energy of a small atomic system with only two Configuration State Functions (CSFs). A similar accuracy was achieved by the full CI method with a much larger number of CSFs. Therefore, it is highly desirable to devise a determinant selection method.

The construction of the Slater part of the wave function (i.e., the selection of the determinants) can be done by Configuration Interaction (CI) or MCSCF type of methods. Here we opted for higher efficiency offered by Selected-CI method [20, 22–25] to build the anti-symmetric component. The Selected-CI method (see Appendix A) enables to pick-up the most significant determinants iteratively from a determinant space which can be generated with significant flexibility on-the-fly. In addition, a faster convergence can be obtained once the single-particle orbitals are also reoptimized in the process. We examined single-electron orbitals generated by different methods in order to have a rapid start into the Selected-CI process.

In order to compare our fixed-node DMC results, we carried out CCSD(T) (i.e., Coupled Cluster, Singles, Doubles with Triples treated approximately) calculations as well. The CCSD(T) results are extrapolated to the complete basis set (CBS) limit which is believed to provide a highly accurate prediction.

The rest of the paper will be organized as follows: the method and computational details will be discussed in Section 2. The results and discussion will be presented in Section 3. Concluding remarks are given in Section 4. Finally, the Selected-CI method is summarized in Appendix A.

2. Method and Computational Details

2.1. Fixed-Node Diffusion Monte Carlo

Diffusion quantum Monte Carlo (DMC) is a projection QMC method in which the ground state of a given symmetry can be obtained by applying the projector operator $e^{-t(H-E_0)}$ to a trial wave function of the same symmetry:

$$\Phi_0 = \lim_{t\to\infty} e^{-t(H-E_0)}\psi_T \tag{2}$$

where Φ_0 and ψ_T are the ground state and trial wave functions, respectively. Therein, H is the Hamiltonian, E_0 is an energy offset and t is a real parameter (imaginary time). Due to the efficiency concerns, one usually prefers the importance sampling, and hence, instead of Eq. 2, the projection takes the following form:

$$f(\mathbf{R}, t+\tau) = \int d\mathbf{R}' \tilde{G}(\mathbf{R} \leftarrow \mathbf{R}', \tau) f(\mathbf{R}', t) \tag{3}$$

where $\tilde{G}(\mathbf{R} \leftarrow \mathbf{R}', \tau)$ is the Green's function, $\mathbf{R}$ and $\mathbf{R}'$ represent electronic configurations and τ is the propagation time step. $f(\mathbf{R}, t)$ is the probability density function which converges to the ground state in the form of $\lim_{t\to\infty} f(\mathbf{R}, t) = \Phi_0(\mathbf{R})\psi_T(\mathbf{R})$. In Eq. 3, the short-time Green's function is given as $\tilde{G}(\mathbf{R} \leftarrow \mathbf{R}', \tau) = \langle \mathbf{R}|e^{-\tau(H-E_0)}|\mathbf{R}'\rangle\, \psi_T(\mathbf{R})\psi_T(\mathbf{R}')^{-1}$. Due to the fermionic nature of wave functions, one faces the well-known fermion sign problem which can be circumvented by using the fixed-node approximation[15, 16, 26–28] among a few prescriptions. In the fixed-node approximation, the sign structure (nodes) of a trial wave function $\psi_T(\mathbf{R})$ is adopted as approximate nodes of the exact wave function $\Phi_0(\mathbf{R})$. This will guarantee that $f(\mathbf{R}, t) \geq 0$ and hence the integral equation introduced in Eq. 3 can now be solved stochastically in an efficient manner. The fixed-node bias which is a consequence of approximate nodes taken from a trial wave function is an important drawback in the application of the fixed-node Diffusion quantum Monte Carlo (FN-DMC), which is otherwise an exact method in principle. The fixed-node error vanishes as the nodes of a trial wave function becomes exact. Although the exact nodes are difficult to estimate except in a few small systems, FN-DMC is known with its high accuracy which can reproduce the experimental results within a marginal error.

2.2. Computational Details

In our calculations, the single-particle orbitals were generated by a hybrid meta-GGA DFT method, TPSSh, with an uncontracted form of the basis sets denoted as *cc-pV5Z-PP*. The core electrons were removed from the calculation by employing the effective core potentials (ECPs) adapted from Ref. [29] so that $4s4p4d5s$ electrons are explicitly considered. The generation of the single-particle orbitals and calculations of the one-body and two-body integrals were done with the quantum Chemistry software package *GAMESS-US* [30]. The one-body and two-body integrals were subsequently exploited in the selected-CI calculations.

The trial wave functions used in our QMC calculations were multi-determinant Slater-Jastrow type wave functions. The Jastrow factor contains electron-nucleus, electron-electron and electron-electron-nucleus terms. The determinant coefficients and the Jastrow function were optimized in the framework of Variational Monte Carlo (VMC) method[31], a variant in the QMC methodology. We observed that the determinant coefficients obtained by a Selected-CI calculation were not always optimum, and therefore, it was essential to re-optimize them with the VMC method.

In addition to FN-DMC, we carried out CCSD(T) calculations with a subsequent extrapolation to the CBS limit. For this purpose, we employed hierarchically designed correlated basis sets, *aug-cc-pV**X**Z-PP*, where $\mathbf{X}$ is the cardinal number of the basis set [29]. We used the uncontracted form of the basis sets and no frozen core was assumed. For the sake of consistency, in both of the QMC and CCSD(T) calculations the same ECPs were preferred. The original pseudopotentials were slightly modified to avoid a potential singularity at nuclei centers which causes large fluctuations in local energy values of QMC. The QMC calculations and CCSD(T) calculations were carried out by using the quantum chemistry packages *QWalk*[32] and *Gaussian09*[33], respectively.

For the CCSD(T)/CBS energy extrapolation we used five schemes[34–38] which will be denoted as CBS_n where $n = 1, 2, .., 5$. The first one, CBS_1, is an exponential scheme[38]:

$$E(\mathbf{X}) = E(\infty) + Ae^{-B\mathbf{X}} \tag{4}$$

where $E(\infty) = E_{cbs}$, $E(\mathbf{X})$ is the energy with a given basis set, and $\mathbf{X}$ is the cardinal number of the basis set. $E(\infty)$, A and B are fitting parameters. The second one, CBS_2, is a power extrapolation scheme[34] given by:

$$E(\mathbf{X}) = E(\infty) + A\mathbf{X}^{-B}, \tag{5}$$

the third one, CBS_3, is a mixed exponential scheme[35]:

$$E(\mathbf{X}) = E(\infty) + Ae^{-(\mathbf{X}-1)} + Be^{-(\mathbf{X}-1)^2}, \tag{6}$$

the fourth one[39], CBS_4, is

$$E(\ell) = E(\infty) + \frac{A}{(\ell + \frac{1}{2})^B}, \tag{7}$$

where ℓ is the maximum angular momentum quantum number in the basis set, and the last one[39], CBS_5, is with integer exponents:

$$E(\ell) = E(\infty) + \frac{A}{(\ell + \frac{1}{2})^4} + \frac{B}{(\ell + \frac{1}{2})^6}. \tag{8}$$

The HF energies were also extrapolated to the CBS limit with the following formula:

$$E_{\mathrm{HF}}(\mathbf{X}) = E_{\mathrm{HF}}(\infty) + A(\mathbf{X}+1)e^{-\gamma\sqrt{\mathbf{X}}} \tag{9}$$

where $E_{\mathrm{HF}}(\infty)$ is the CBS limit of the Hartree-Fock (HF) energy, and $E_{\mathrm{HF}}(\infty)$, A and γ are fitting parameters.

We should also note that all calculations were done at the experimental bond length, i.e., 1.93 Å [9].

3. Results and Discussion

The DMC and VMC energies of the dimer state (Mo_2) with respect to the number of determinants in the trial wave function are given in Fig. 1. The percentages of the correlation energy recovered by DMC to the estimated exact correlation energy are also presented in the same figure. The estimation of the exact energy of the dimer state was based on the atomic DMC energy, the experimental value for the binding energy (4.29(2) eV) and the estimated zero-point-energy (0.03 eV). This is, however, a biased estimation as the experimental reports in the literature do not imply a clear consistency among each other (see Table 2). Despite this, such an estimation can still be helpful to depict the performence of our calculations.

The number of determinants was up to 3500. The DMC energy apparently converged to a value with respect to the number of determinants. We observed that a further noticeable energy drop was only possible if a substantially high number of additional determinants were considered in the trial wave function. This is because the energy contribution of determinants selected iteratively by the Selected-CI method drops in a geometric fashion as the number of determinants increases. Hence, the expansion of initial determinants is relatively easy to optimize. However, as the expansion of the determinants grows, the wave function will contain many determinants with low energy contributions, thereby making the optimization more challenging.

A faster convergence can be reached by exploiting higher quality single-particle orbitals. After examining orbitals generated by different techniques such as HF orbitals, natural orbitals generated by CISD with various virtual orbital spaces and DFT orbitals, we observed that DFT orbitals provide lower energies. Also, among many types of functionals, TPSSh,which is a hybrid meta-GGA DFT functional, was found to yield slightly better orbitals.

The same optimization procedure was followed for the atomic state as well. Since the error cancellation – i.e., mainly the fixed-node error cancellation in our case– plays a crucial role in energy difference calculations, it was important to treat the atomic and dimer states on an equal footing. However, unlike the dimer that is well-known to have a highly multi-reference wave function, the atomic state is dominated by a single-reference and hence the optimization yielded very small multi-reference expansion coefficients. Therefore, the atomic multi-determinant wave function resulted only in negligible total energy improvements.

Nevertheless, as it is given in Fig. 1, the DMC calculation of Mo_2 with 3500 determinants gained a high percentage, 98.20(3)%, of the correlation energy.

In Table 1, the CCSD(T) and HF energies calculated with the correlation-consistent basis sets, aug-cc-pV**X**Z-PP, and their extrapolations to the CBS limit according to the aforementioned schemes are given. In Fig. 2, the extrapolation of the HF energies of Mo and Mo_2 following the scheme given in Eq. 9 is presented. The CBS extrapolations of the CCSD(T) energies of Mo and Mo_2 according to the five schemes

introduced in Eqs. 4-8 are shown in Figs. 3 and 4, respectively. The binding energies calculated by the DMC and CCSD(T) methods are presented in Table 2. In addition to the current work, other theoretical and experimental reports in the literature are also given in the same table. One can notice that the binding energies shown in Table 2 are calculated method-consistently; i.e., the energies of Mo and Mo_2 are considered in the same level of method.

It is remarkable that although the DMC method provides lower energies than CCSD(T)/aug-pV**X**Z-PP does in both of the atomic and dimer states, the binding energies obtained by CCSD(T)/aug-pV**X**Z-PP are closer to the experimental values than DMC/MDSJ (DMC with a multi-determinant Slater-Jastrow type trial wave function) is. This indicates that the error cancellation is in favor of the CCSD(T)/aug-pV**X**Z-PP method compared to DMC/MDSJ. One can deduce that the balance of the fixed-node DMC biases is less even in different systems and this is well-known to cause increase in the corresponding bias, see for example Ref. [40]. Arguably, Mo dimer is a case where this aspect comes to the forefront due to the significant differences between single-reference vs. multi-reference wave functions of atomic vs. dimer states, respectively. This can be partially alleviated by improving the trial wave functions as presented here. Clearly, one of our goals was to shed some light on how effective the multi-reference expansions with medium size of the excitation space can be for these types of systems. The corresponding binding energies calculated by the fixed-node DMC method with an increasing number of determinants are presented in Table 3.

The CBS extrapolation aims at lifting the bias introduced due to the truncated basis sets. CCSD(T)/CBS energies in both Mo and Mo_2 are lower than DMC/MDSJ energies. The main reason for this missing correlation energy in DMC/MDSJ is the fixed-node bias. The fixed-node bias can vanish if the trial wave function nodes are the same as the nodes of the exact wave function. Such a wave function, in principle, could be constructed if we were able to optimize and run a complete set of determinants; albeit this is not possible. In other words, similar to the bias originating from the finite basis set in CCSD(T), DMC suffers from the fixed-node bias which is indirectly associated with the finite set of determinants in our specific case. The unfortunate point for the DMC method is that unlike well-developed systematic extrapolation schemes to the CBS limit in CCSD(T)/aug-pV**X**Z-PP, there is no such a fully developed method that would extrapolate DMC energies from finite numbers of the determinants to the infinite number of determinants.

CCSD(T)/CBS methods provide binding energies with a satisfactory agreement with the experimental values. DMC, however, underestimates the binding energy by almost 0.5-0.7 eV. On the other hand, the binding energy can be a misleading quantity to compare the accuracy of the methods due to error cancellations. It is known that DMC and CCSD(T) are competitive methods which can produce results with a similar accuracy. Nevertheless, the well-developed CBS extrapolation schemes deliver a systematic advantage to CCSD(T)/CBS. From a feasibility point of view, however, DMC is much more practical than CCSD(T) due to the time scaling and parallelism in QMC. As the system size increases CCSD(T) is simply ruled out.

Mo_2, with d-d bondings, was expected to pose a great challenge for the fixed-node DMC. This is because the fixed-node bias increases with electron density and non-linearity on nodal surface[40] which are presumably abundant in d-d bondings. One of the remedies is to employ a multi-referenced trial wave function of a high quality. As shown in Table 1, DMC recovers almost 98% of the correlation energy which is, in fact, an indicator of high quality of the trial wave functions constructed. However, the missing 2% of the correlation energy has a significant importance. In order to recover the missing correlation energy, one can construct the trial wave functions with a better set of single-particle orbitals than the ones we have already examined in this study or construct the trial wave function by including more determinants. As we discussed above, the latter will be, however, beyond the feasibility of the calculations since it will require a much higher number of determinants most of which are with small contribution to the energy.

4. Conclusion

In this paper, we presented our study on the molybdenum dimer. We calculated the binding energy of Mo_2 at the experimental bond length by means of the fixed-node DMC method. The multi-determinant Slater component of the trial wave function was constructed by employing the Selected-CI method. It helps to include all possible highly contributing determinants iteratively so that the wave function contains only

the most relevant determinants, thereby making the wave function as compact as possible. As QMC is a computationally demanding method, Selected-CI can be considered as an efficient tool in constructing a trial wave function.

We also compared our DMC results with the results obtained by the CCSD(T) method which is usually seen as the golden standard in the Quantum Chemistry community. DMC was able to provide lower energies in both the atomic and dimer states than CCSD(T)/aug-pV**X**Z-PP. However, with the favorable error cancellations the binding energies obtained by CCSD(T)/aug-pV**X**Z-PP were closer to the experimental value than the DMC binding energy result was. Furthermore, the well-developed CBS extrapolation schemes enable a systematic estimation of the CBS limit out of the truncated basis set results of CCSD(T). In our study, the CCSD(T)/CBS results with various extrapolation schemes yield a reasonable agreement with the experimental values. Nonetheless, FN-DMC with a multi-Slater determinant trial wave function was able to recover a high percentage of correlation energies.

Appendix A Selected-CI method

The construction of a multi-determinant trial wave function in QMC is usually done by selecting the determinants according to the absolute values of expansion coefficients. An alternative way can be to select the determinants considering their energy contributions via the Selected-CI method. This can be more efficient strategy to keep the wave function as compact as possible.

By beginning with the HF determinant, the most optimum determinants are selected iteratively. Let $K^{(n)}$ be the subspace of determinants at the iteration n and also let $|\Psi^{(n)}\rangle$ be the corresponding eigenstate with the lowest eigenvalue of the Hamiltonian

$$H \leftarrow H_{ij} = \langle D_i|H|D_j\rangle \qquad for \quad |D_i\rangle\,, |D_j\rangle \in K^{(n)}. \tag{10}$$

where $|D_i\rangle$ is a Slater determinant in the subspace $K^{(n)}$. Hence, the wave function will be a linear combination of the Slater determinants in the subspace:

$$|\Psi^{(n)}\rangle = \sum_{\substack{i \\ |D_i\rangle \in K^{(n)}}} c_i^{(n)} |D_i\rangle. \tag{11}$$

The Selected-CI algorithm can be summarized as follows:
i) One can begin with the HF determinant and expand the wave function iteratively. ii) At the iteration n, generate a universal space K_u^n of excited determinants of $|\Psi^{(n-1)}\rangle$; a determinant pool. This is performed by applying singly excitation and doubly excitation operators on each determinant in $K^{(n-1)}$. One may prefer some restrictions in the generation of determinants since the number of excited determinants may reach a prohibitive level.

iii) Scan each determinant in $K_u^{(n)}$ which does not exist in $K^{(n-1)}$ and find the coupling of each determinant with $|\Psi^{(n-1)}\rangle$:

$$H_{i(n-1)} = \langle D_i|H|\Psi^{(n-1)}\rangle \tag{12}$$

where $D_i \notin K^{(n-1)}$ but $D_i \in K_u^{(n)}$. If the coupling is non-zero, then the energy contribution is calculated according to Epstein-Nesbet perturbation theory:

$$\Delta E_i = \frac{|\langle D_i|H|\Psi^{(n-1)}\rangle|^2}{E^{(n-1)} - E_{ii}} = \frac{H_{i(n-1)}^2}{E^{(n-1)} - E_{ii}} \tag{13}$$

where $E_{ii} = \langle D_i|H|D_i\rangle$ and $E^{(n)} = \langle\Psi^{(n)}|H|\Psi^{(n)}\rangle$ are the self-energies of the particular determinant and the current wave function, respectively. It is noteworthy that the determinants are normalized, i.e., $\langle D_i|D_j\rangle = \delta_{ij}$ and $H_{ij} = \langle D_i|H|D_j\rangle$ is calculated according to Slater-Condon rules.
iv) The determinant with the lowest ΔE_i is taken into the subspace:

$$K^{(n-1)} + |D_\zeta\rangle \rightarrow K^{(n)}$$

Mo			
Basis Set	**CCSD(T) En. (Ha)**	**HF En. (Ha)**	**Corr. En. (Ha)**
aug-pVTZ-PP	-67.7595	-67.3423	0.4172
aug-pVQZ-PP	-67.8108	-67.3424	0.4684
aug-pV5Z-PP	-67.8334	-67.3424	0.4910
CBS_1	-67.8513	-67.3424	0.5089
CBS_2	-67.8695	-67.3424	0.5271
CBS_3	-67.8466	-67.3424	0.5042
CBS_4	-67.8628	-67.3424	0.5204
CBS_5	-67.8596	-67.3424	0.5172
	En. (Ha)		**Corr. En.(Ha)**
DMC/MDSJ/SDSJ*	-67.8455(5)		0.5031(5)
Mo_2			
Basis Set	**CCSD(T) En. (Ha)**	**HF En. (Ha)**	**Corr. En. (Ha)**
aug-pVTZ-PP	-135.6529	-134.3379	1.3150
aug-pVQZ-PP	-135.7640	-134.3408	1.4232
aug-pV5Z-PP	-135.8127	-134.3415	1.4712
CBS_1	-135.8505	-134.3417	1.5089
CBS_2	-135.8889	-134.3417	1.5471
CBS_3	-135.8411	-134.3417	1.4994
CBS_4	-135.8748	-134.3417	1.5331
CBS_5	-135.8686	-134.3417	1.5270
	En. (Ha)		**Corr. En. (Ha)**
DMC/SDSJ	-135.7993(4)		1.4576(4)
DMC/MDSJ	-135.8229(3)		1.4812(3)

Table 1: The CCSD(T) and DMC energies of Mo and Mo_2 are given. The CBS extrapolation methods denoted as CBS_n where $n = 1, 2, ..., 5$ are explained in the text (see Eqs. 4-8). DMC/SDSJ and DMC/MDSJ stand for DMC calculations with single-determinant and multi-determinant trial wave functions, respectively.
*DMC/MDSJ/SDSJ indicates that the DMC/MDSJ and DMC/SDSJ yield esentially the same energy value in the atomic state. This was because the difference between the DMC/SDSJ and DMC/MDSJ energies in the atomic state (Mo) was negligible within the error bars.

where D_ζ is the determinant such that $\Delta E_\zeta = min(\{\Delta E_i\})$.
v) The hamiltonian matrix, H_{ij}, is formed and diagonalized with the determinants in the new subspace $K^{(n)}$ which yields a new wave function $\Psi^{(n)}$ and the energy $E^{(n)}$
vi) Go to step ii) and repeat the steps until the size of the wave function or convergence in the energy reaches the desired value.

So far we have only pronounced determinants. However, a determinant is not a pure spin state, therefore, a selection scheme based on determinants may result in spin contamination. In order to avoid spin contamination, CSFs which are appropriate linear combinations of a number of determinants yielding pure spin states may be preferred. Switching to CSFs will also lower the number of functions in the universal determinant (now CSF) space.

References

[1] K. Andersson, B. O. Roos, P. Malmqvist, P.-O. Widmark, The Cr_2 potential energy curve studied with multiconfigurational second-order perturbation theory, Chem. Phys. Lett. 230 (1994) 391–397.

Method	$\mathbf{D_0}$**(eV)**	R_e/Å
MRSDCI+Q [6]	2.92	1.993
CASSCF [14]	0.55	2.10
CASPT2 [14]	2.14	2.09
PNOF5 [14]	3.26	2.10
CASSCF/MS-CASPT2 [8]	4.41	1.95
AFQMC/CASSCF/CBS [41]	4.46(5)	1.95(2)
CCSD(T)/aug-pVTZ-PP (this work)	3.61	1.93
CCSD(T)/aug-pVQZ-PP (this work)	3.84	1.93
CCSD(T)/aug-pV5Z-PP (this work)	3.94	1.93
CCSD(T)/CBS_1 (this work)	4.00	1.93
CCSD(T)/CBS_2 (this work)	4.05	1.93
CCSD(T)/CBS_3 (this work)	3.99	1.93
CCSD(T)/CBS_4 (this work)	4.03	1.93
CCSD(T)/CBS_5 (this work)	4.04	1.93
DMC/SDSJ (this work)	2.92(3)	1.93
DMC/MDSJ (this work)	3.56(3)	1.93
exp. [42]	4.29(2), 4.2(3)	
exp. [43]	4.47(1)	
exp. [13]	4.1(7)	1.93
exp. [44]		1.93
exp. [45]		1.94

Table 2: The binding energies of Mo_2 obtained by several methods are shown. The CBS extrapolation methods denoted as CBS_n where $n = 1, 2, ..., 5$ are explained in the text (see Eqs. 4-8). DMC/SDSJ and DMC/MDSJ stand for DMC calculations with single-determinant and multi-determinant trial wave functions, respectively.

$\mathbf{N_{Det}}$	$\mathbf{D_0}$**(eV)**
1	2.92(3)
4	3.07(3)
22	3.20(3)
300	3.43(3)
600	3.45(4)
1200	3.49(3)
2400	3.53(3)
3000	3.55(3)
3500	3.56(3)

Table 3: The DMC binding energies of the molybdenum dimer calculated with an increasing number of determinants in the trial wave function of a Slater-Jastrow type are given.

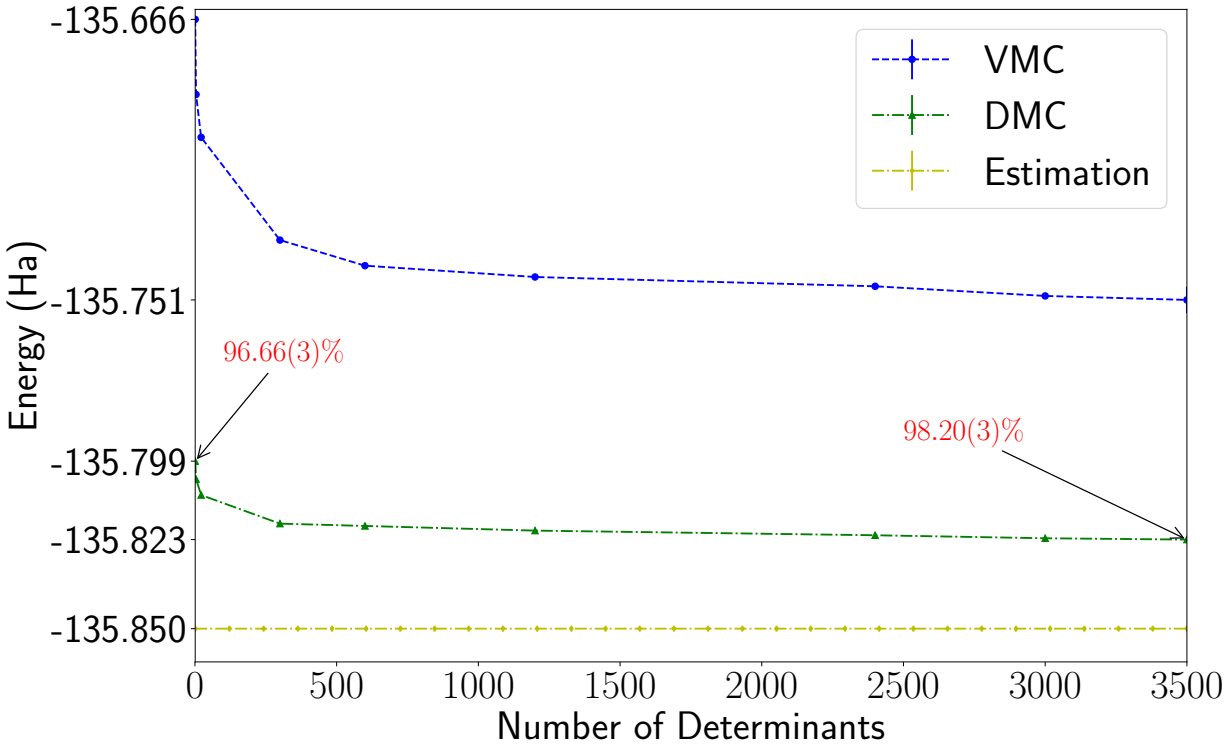

Figure 1: Mo_2 energy obtained by the DMC and VMC methods with a varying number of determinants are given. The estimated exact energy is based on the DMC energy of Mo, the experimental binding energy value, 4.29(2) eV, and an estimated value of the zero-point-energy, 0.03 eV. Note that this is a biased estimation as there are discrepancies among different experimental reports in the literature (see Table 2). The error bars for the VMC and DMC energies are much smaller than the scale of the graph.

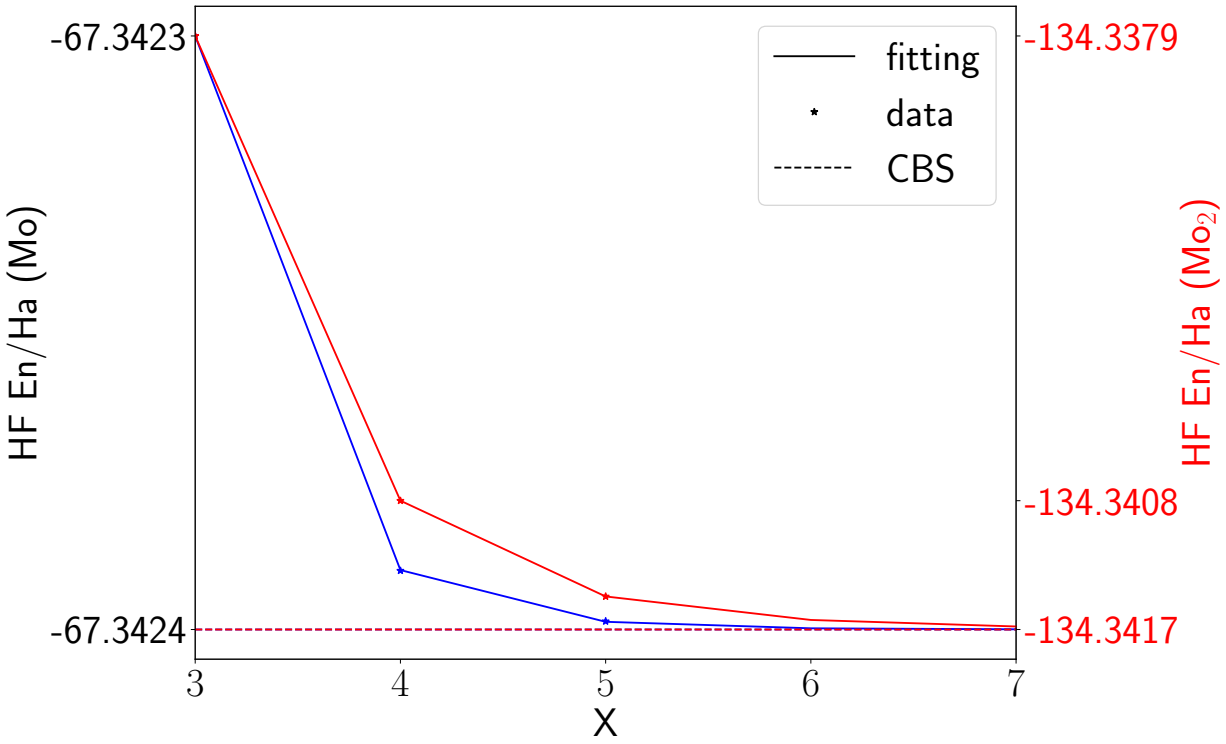

Figure 2: The CBS extrapolations of the HF energies of the Mo (left) and Mo_2 (right) systems obtained with the basis sets aug-pV**X**Z-PP are shown. The extrapolation scheme given in Eq. (9) is employed.

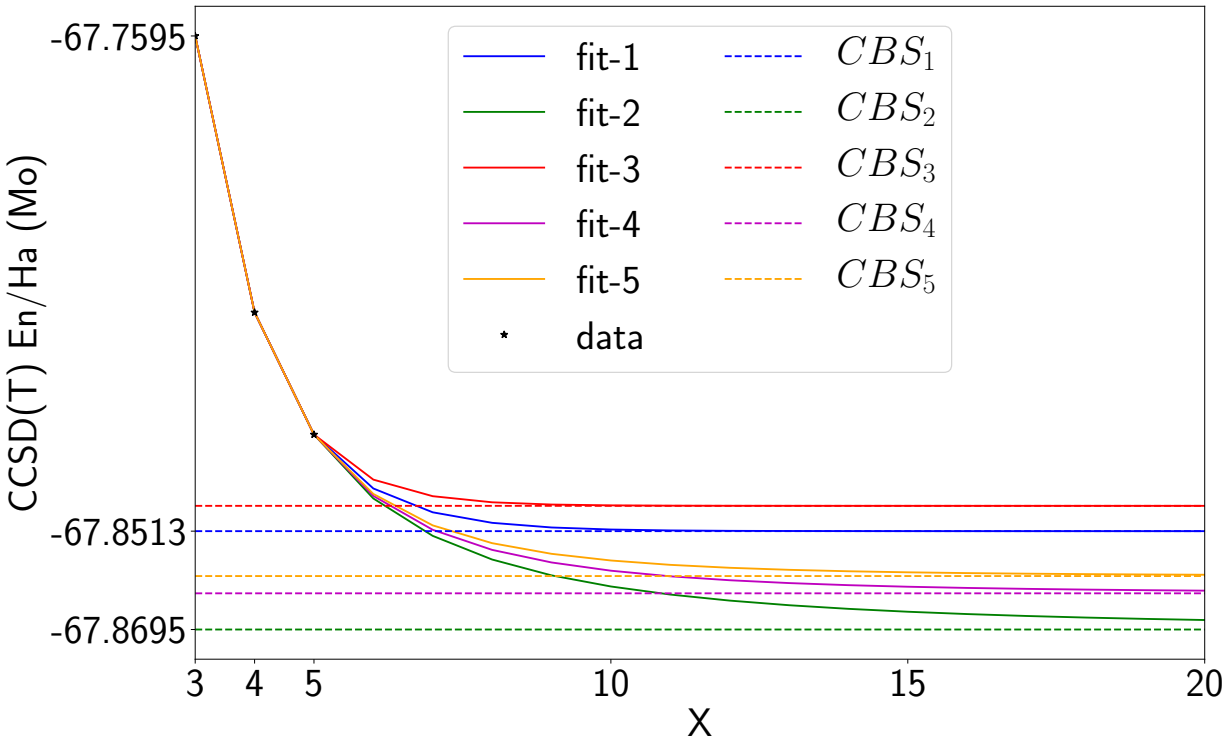

Figure 3: The CBS extrapolations of the energies of Mo obtained by the CCSD(T)/aug-pV**X**Z-PP method are shown. Various extrapolation schemes given in Eqs. (4-8) are exploited. The fittings and CBS limits are presented.

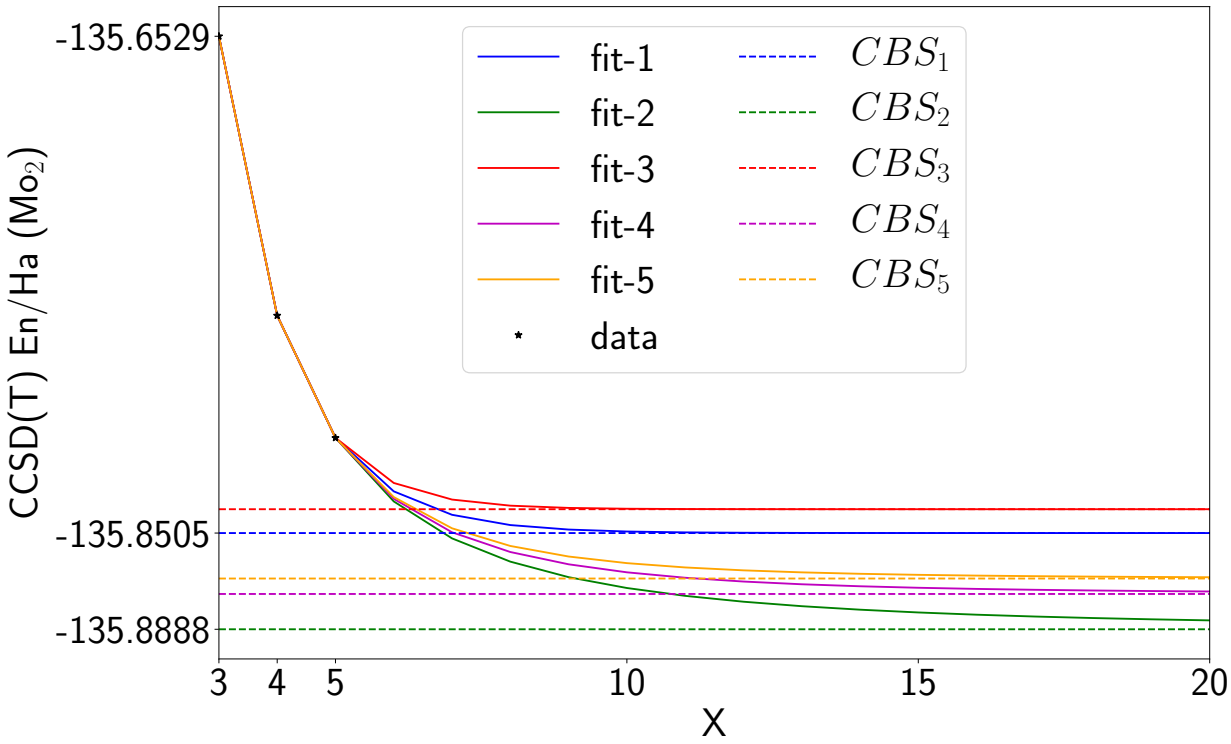

Figure 4: The CBS extrapolations of the energies of Mo_2 obtained by the CCSD(T)/aug-pV**X**Z-PP method are shown. Various extrapolation schemes given in Eqs. (4-8) are exploited. The fittings and CBS limits are presented.

[2] H. Dachsel, R. J. Harrison, D. A. Dixon, Multireference Configuration Interaction Calculations on Cr_2 : Passing the One Billion Limit in MRCI/MRACPF Calculations, J. Phys. Chem. A 2 (1999) 152–155.
[3] K. Hongo, R. Y. O. Maezono, A Benchmark Quantum Monte Carlo Study of the Ground State Chromium Dimer, Int. J. Quantum Chem. 112 (2012) 1243–1255.
[4] D. L. Michalopoulos, D. E. Powers, R. E. Smalley, The Bond Length of Cr_2, J. Phys. Chem. 86 (1982) 3914–3916.
[5] T. Müller, Large-Scale Parallel Uncontracted Multireference-Averaged Quadratic Coupled Cluster : The Ground State of the Chromium Dimer Revisited, J. Phys. Chem. A 113 (2009) 12729–12740.
[6] K. Balasubramanian, Spectroscopic properties of Mo_2^- and Mo_2^+, Chem. Phys. Lett. 365 (2002) 413–420.
[7] K. Balasubramanian, X. Zhu, Spectroscopic constants and potential energy curves of electronic states of Mo_2, J. Chem. Phys. 117 (10) (2002) 4861. doi:10.1063/1.1497641.
[8] A. C. Borin, J. P. Gobbo, B. O. Roos, A theoretical study of the binding and electronic spectrum of the Mo_2 molecule, Chem. Phys. 343 (2-3) (2008) 210–216. doi:10.1016/j.chemphys.2007.05.028.
[9] Y. M. Efremov, V. B. Kozhukhovsky, L. V. Gurvich, On the Electronic Spectrum of the Mo_2 Molecule Observed after Flash Photolysis of $Mo(CO)_6$, J. Mol. Spectrosc. 440 (1978) 430–440.
[10] M. M. Goodgame, W. A. Goddard, Nature of Mo-Mo and Cr-Cr Multiple Bonds: A Challenge for the Local-Density Approximation, Phys. Rev. Lett. 48 (1982) 135–138.
[11] P. Atha, I. Hillier, M. Guest, Correlation effects in the ground and ionic states of $Mo_2(O_2CH)_4$ and $Cr_2(O_2CH)_4$, Mol. Phys. 46 (2) (1982) 437–448. doi:10.1080/00268978200101311.
[12] N. A. Baykara, B. N. Mcmaster, D. R. Salahub, LCAO local-spin-density and Xα calculations for Cr_2 and Mo_2, Mol. Phys. 52 (4) (1984) 891–905.
[13] W. Zhang, X. Ran, H. Zhao, L. Wang, The nonmetallicity of molybdenum clusters, The Journal of Chemical Physics 121 (16) (2004) 7717. doi:10.1063/1.1790911.
[14] F. Ruiperez, M. Piris, J. M. Ugalde, J. M. Matxain, The natural orbital functional theory of the bonding in Cr_2, Mo_2 and W_2, Phys. Chem. Chem. Phys. 15 (2013) 2055–2062. doi:10.1039/c2cp43559d.
[15] J. Kolorenč, L. Mitas, Applications of quantum Monte Carlo methods in condensed systems, Reports Prog. Phys. 74 (2) (2011) 026502. doi:10.1088/0034-4885/74/2/026502.
[16] W. Foulkes, L. Mitas, R. Needs, G. Rajagopal, Quantum Monte Carlo simulations of solids, Rev. Mod. Phys. 73 (1) (2001) 33–83. doi:10.1103/RevModPhys.73.33.
[17] B. M. Austin, D. Y. Zubarev, W. A. Lester Jr., Quantum Monte Carlo and Related Approaches, Chem. Rev. 112 (2012) 263–288.
[18] B. L. Hammond, W. A. Lester, P. J. Reynolds, Monte Carlo Methods in Ab Initio Quantum Chemistry, WORLD SCIENTIFIC, ISBN:978-981-02-0321-4, 1994. doi:10.1142/1170.
URL https://www.worldscientific.com/doi/abs/10.1142/1170
[19] P. K. V. V. Nukala, P. R. C. Kent, A fast and efficient algorithm for Slater determinant updates in quantum Monte Carlo simulations., J. Chem. Phys. 130 (20) (2009) 204105. doi:10.1063/1.3142703.
[20] E. Giner, A. Scemama, M. Caffarel, Fixed-node diffusion Monte Carlo potential energy curve of the fluorine molecule F_2 using selected configuration interaction trial wavefunctions, Journal of Chemical Physics 142 (4) (2015). doi:10.1063/1.4905528.
[21] A. H. Kulahlioglu, K. Rasch, S. Hu, L. Mitas, Density dependence of fixed-node errors in diffusion quantum Monte Carlo: Triplet pair correlations, Chem. Phys. Lett. 591 (2014) 170–174. doi:10.1016/j.cplett.2013.11.033.
[22] E. Giner, A. Scemama, M. Caffarel, Using perturbatively selected configuration interaction in quantum Monte Carlo calculations, Can. J. Chem. 91 (9) (2013) 879–885.
[23] M. Dash, J. Feldt, S. Moroni, A. Scemama, C. Filippi, Excited states with selected CI-QMC: chemically accurate excitation energies and geometries, arXiv e-prints (2019) arXiv:1905.06737.
[24] M. Dash, S. Moroni, A. Scemama, C. Filippi, Perturbatively Selected Configuration-Interaction Wave Functions for Efficient Geometry Optimization in Quantum Monte Carlo, Journal of Chemical Theory and Computation 14 (8) (2018) 4176–4182. doi:10.1021/acs.jctc.8b00393.
[25] M. Caffarel, T. Applencourt, E. Giner, A. Scemama, Communication: Toward an improved control of the fixed-node error in quantum Monte Carlo: The case of the water molecule, Journal of Chemical Physics 144 (15) (2016). doi:10.1063/1.4947093.
[26] J. B. Anderson, Quantum chemistry by random walk. H 2P, H+3 D3h 1A'1, H2 $3\Sigma+u$, H4 $1\Sigma+g$, Be 1S, J. Chem. Phys. 65 (10) (1976) 4121–4127. doi:10.1063/1.432868.
[27] P. J. Reynolds, D. M. Ceperley, B. J. Alder, W. A. Lester, Jr., Fixed-node quantum Monte Carlo for molecules , J. Chem. Phys. 77 (11) (1982) 5593–5603. doi:10.1063/1.443766.
[28] D. J. Klein, Nodal hypersurfaces and Anderson's random-walk simulation of the Schr odinger equation, J. Chem. Phys. 64 (11) (1976) 4811. doi:10.1063/1.432043.
[29] K. A. Peterson, D. Figgen, M. Dolg, H. Stoll, Energy-consistent relativistic pseudopotentials and correlation consistent basis sets for the 4d elements Y-Pd., J. Chem. Phys. 126 (12) (2007) 124101. doi:10.1063/1.2647019.
[30] M. S. Gordon, M. W. Schmidt, LATER, in: C. E. Dykstra, K. S. Kim, G. E. Scuseria (Eds.), Theory Appl. Comput. Chem. first forty years, Elsevier, Amsterdam, 2005, Ch. Advances i, pp. 1167–1189.
[31] C. Umrigar, C. Filippi, Energy and Variance Optimization of Many-Body Wave Functions, Phys. Rev. Lett. 94 (15) (2005) 150201. doi:10.1103/PhysRevLett.94.150201.
[32] L. K. Wagner, M. Bajdich, L. Mitas, QWalk: A quantum Monte Carlo program for electronic structure, J. Comput. Phys. 228 (9) (2009) 3390–3404. doi:10.1016/j.jcp.2009.01.017.
[33] M. J. Frisch, G. W. Trucks, H. B. Schlegel, *et al.*, Gaussian 09 Revision D.01, Gaussian Inc., Wallingford CT, 2009.

[34] T. Helgaker, W. Klopper, H. Koch, J. Noga, Basis-set convergence of correlated calculations on water, J. Chem. Phys. 106 (23) (2002) 9639–9646. doi:10.1063/1.473863.

[35] D. E. Woon, T. H. Dunning, Benchmark calculations with correlated molecular wave functions. VI. Second row A2 and first row/second row AB diatomic molecules, J. Chem. Phys. 101 (10) (1994) 8877–8893. doi:10.1063/1.468080.

[36] V. Vasilyev, Online complete basis set limit extrapolation calculator, Comput. Theor. Chem. 1115 (2017) 1–3. doi:10.1016/j.comptc.2017.06.001.

[37] A. Karton, J. M. L. Martin, Comment on: "Estimating the Hartree–Fock limit from finite basis set calculations" [Jensen F (2005) Theor Chem Acc 113:267], Theor. Chem. Acc. 115 (4) (2006) 330–333. doi:10.1007/s00214-005-0028-6.

[38] D. Feller, Application of systematic sequences of wave functions to the water dimer, J. Chem. Phys. 96 (8) (1992) 6104–6114. doi:10.1063/1.462652.

[39] J. M. L. Martin, Ab initio total atomization energies of small molecules - towards the basis set limit, Chem. Phys. Lett. 259 (September) (1996) 669–678.

[40] K. M. Rasch, S. Hu, L. Mitas, Communication: Fixed-node errors in quantum Monte Carlo: Interplay of electron density and node nonlinearities, J. Chem. Phys. 140 (4) (2014) 041102. doi:10.1063/1.4862496.

[41] W. Purwanto, S. Zhang, H. Krakauer, Auxiliary-field quantum monte carlo calculations of the molybdenum dimer, J. Chem. Phys. 144 (24) (2016) 244306. doi:10.1063/1.4954245.

[42] S. K. Gupta, R. M. Atkins, K. A. Gingerich, Mass Spectrometric Observation and Bond Dissociation Energy of Dimolybdenum , Mo_2(g), Inorg. Chem. 17 (11) (1978) 3111–3213.

[43] B. Simard, M.-A. Lebeault-Dorget, A. Marijnissen, J. J. ter Meulen, Photoionization spectroscopy of dichromium and dimolybdenum: Ionization potentials and bond energies, J. Chem. Phys. 108 (23) (1998) 9668. doi:10.1063/1.476442.

[44] M. J. Pellin, T. Foosnaes, D. M. Gruen, Fluorescence spectrum of Mo_2 in argon and krypton matrices, J. Chem. Phys. 74 (10) (1981) 5547. doi:10.1063/1.440917.

[45] J. B. Hopkins, P. R. R. LangridgeSmith, M. D. Morse, R. E. Smalley, Supersonic metal cluster beams of refractory metals: Spectral investigations of ultracold Mo_2, J. Chem. Phys. 78 (4) (1983) 1627. doi:10.1063/1.444961.

Acknowledgement

This research was supported by the Department of Energy, Office of Basic Energy Sciences, Division of Materials Science and Engineering grant DE-SC0012314.